JGP Journal of General Physiology

RESEARCH ARTICLE

Four drug-sensitive subunits are required for maximal effect of a voltage sensor–targeted KCNQ opener

Alice W. Wang[1], Michael C. Yau[1,2], Caroline K. Wang[1], Nazlee Sharmin[1], Runying Y. Yang[1], Stephan A. Pless[2], and Harley T. Kurata[1]

KCNQ2-5 (Kv7.2–Kv7.5) channels are strongly influenced by an emerging class of small-molecule channel activators. Retigabine is the prototypical KCNQ activator that is thought to bind within the pore. It requires the presence of a Trp side chain that is conserved among retigabine-sensitive channels but absent in the retigabine-insensitive KCNQ1 subtype. Recent work has demonstrated that certain KCNQ openers are insensitive to mutations of this conserved Trp, and that their effects are instead abolished or attenuated by mutations in the voltage-sensing domain (VSD). In this study, we investigate the stoichiometry of a VSD-targeted KCNQ2 channel activator, ICA-069673, by forming concatenated channel constructs with varying numbers of drug-insensitive subunits. In homomeric WT KCNQ2 channels, ICA-069673 strongly stabilizes an activated channel conformation, which is reflected in the pronounced deceleration of deactivation and leftward shift of the conductance–voltage relationship. A full complement of four drug-sensitive subunits is required for maximal sensitivity to ICA-069673—even a single drug-insensitive subunit leads to significantly weakened effects. In a companion article (see Yau et al. in this issue), we demonstrate very different stoichiometry for the action of retigabine on KCNQ3, for which a single retigabine-sensitive subunit enables near-maximal effect. Together, these studies highlight fundamental differences in the site and mechanism of activation between retigabine and voltage sensor–targeted KCNQ openers.

Introduction

Voltage-gated potassium channels in the KCNQ gene family exhibit unique features of physiological and pharmacological modulation (Miceli et al., 2008; Barrese et al., 2018). Similar to other Kv channel types, they respond to changes in membrane voltage through a canonical voltage-sensing domain (VSD; Miceli et al., 2009, 2011). They are also regulated by membrane PIP2 content, and depletion of PIP2 by receptor-coupled second messenger systems (usually signaling through Gq and phospholipase C) attenuates channel activity and increases cellular electrical excitability (Delmas and Brown, 2005; Suh et al., 2006; Suh and Hille, 2007). KCNQ channels are especially unique because of their sensitivity to a diverse set of small molecules that can profoundly enhance channel activity (Miceli et al., 2017; Barrese et al., 2018).

The most widely studied KCNQ channel opener is retigabine, a drug that has been approved for use in humans as an antiepileptic drug and has been explored for other therapeutic applications (Porter et al., 2007; Mackie and Byron, 2008; Brodie et al., 2010; Wainger et al., 2014). However, there is growing recognition that small-molecule activators of KCNQ channels can act through a variety of molecular mechanisms. Retigabine is thought to bind to a Trp side chain conserved in the pore-forming S5 segments of KCNQ2–5 channels, leading to a stabilization of channel opening that is reflected in a shift of channel activation to more negative voltages, acceleration of activation kinetics, and deceleration of channel closure (Schenzer et al., 2005; Lange et al., 2009; Kim et al., 2015; Yau et al., 2018). Although many KCNQ channel openers rely on this conserved Trp (Bentzen et al., 2006; Yu et al., 2011), a second category of compounds appears to target the voltage-sensing domain, often with greater KCNQ subtype selectivity than retigabine (Padilla et al., 2009; Wang et al., 2017). Several reports have described KCNQ activators that are insensitive to mutation of the conserved pore-domain Trp side chain required for retigabine activity (Xiong et al., 2007; Gao et al., 2010; Peretz et al., 2010; Li et al., 2013), and chimeric studies have demonstrated that the sensitivity to certain KCNQ openers is determined by the VSD (Padilla et al., 2009; Peretz et al., 2010; Li et al., 2013). Recent work from our group identified two specific amino acid positions in the S3 segment of the KCNQ2 VSD (A181 and F168) that are required for sensitivity to the benzamide ICA-069673 (ICA73) and appear to partially determine the strong specificity of this drug for KCNQ2 over KCNQ3 (Wang et al., 2017).

The remarkable diversity of compounds with KCNQ channel–activating properties, and the apparent diversity of channel segments that control sensitivity to these various drugs, sug-

[1]Department of Pharmacology, Alberta Diabetes Institute, University of Alberta, Edmonton, AB, Canada; [2]Drug Design and Pharmacology (Center for Biopharmaceuticals), University of Copenhagen, Copenhagen, Denmark.

Correspondence to Harley T. Kurata: kurata@ualberta.ca.

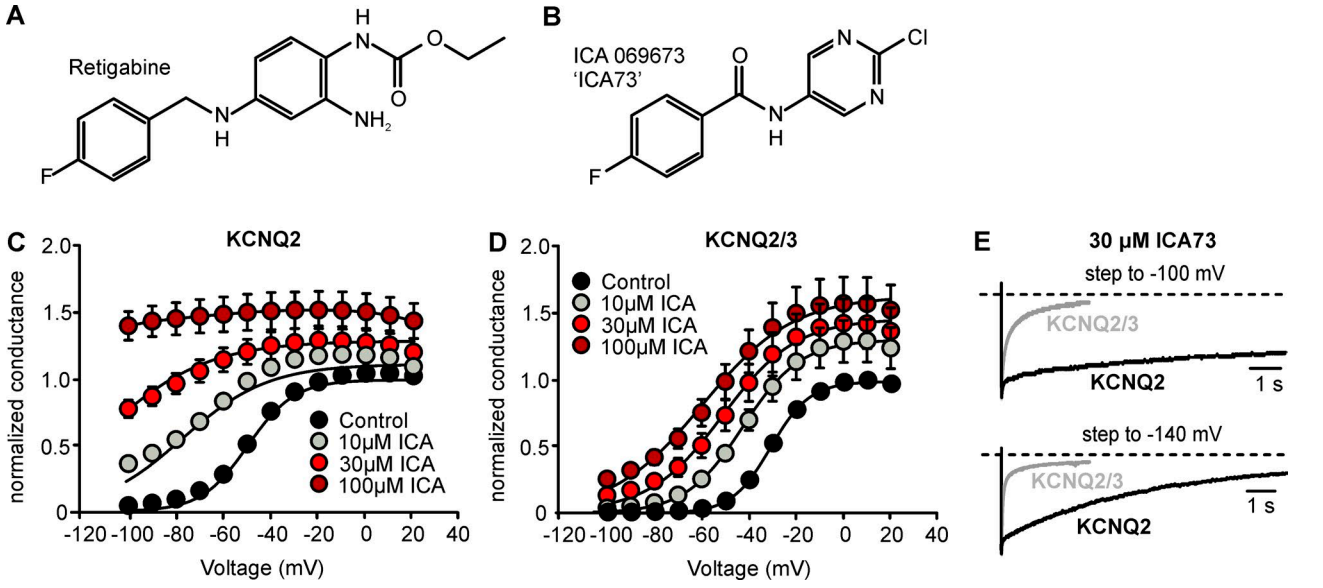

Figure 1. **ICA73 effects depend on KCNQ channel subunit composition. (A and B)** Conductance–voltage relationships were constructed for homomeric KCNQ2 or heteromeric KCNQ2/3 channels expressed in *X. laevis* oocytes. Injected oocytes were held at −100 mV and pulsed for 2 s between voltages of +20 and −100 mV, followed by a test pulse to −20 mV (start-to-start interval, 5 s). **(C and D)** Conductance–voltage relationships were generated by normalizing tail current magnitude to the peak tail current observed in control conditions. **(E)** Tail current kinetics of homomeric KCNQ2 or heteromeric KCNQ2/3 channels in the presence of 30 μM ICA73, elicited by a step to −100 mV after a prepulse to +20 mV. Error bars are mean ± SEM.

gests that deeper investigation of the mechanism of action and binding of KCNQ activator compounds is required. We sought to further investigate the molecular mechanism of action of voltage sensor–targeted KCNQ channel openers by determining the subunit stoichiometry of their effects. Building on our recent identification of KCNQ2 A181 and F168 as essential side chains for ICA73 effects, we generated KCNQ2 channels with defined numbers of ICA73-insensitive subunits by building concatenated tetrameric constructs. By varying the number of A181P and F168L subunits in the functional tetramer, we determined the number of ICA73-sensitive subunits required to generate full channel gating sensitization. Our findings demonstrate that a full complement of four available ICA73-sensitive subunits is required to generate the maximal drug effect, although even a single insensitive subunit leads to a significant drop in ICA73 sensitivity. This stoichiometric requirement for voltage sensor–targeted KCNQ channel openers explains the disparity between their effects on homomeric KCNQ2 channels versus heteromeric KCNQ2/3 channels and highlights their distinct mechanism of action compared with pore-targeted openers such as retigabine.

Materials and methods

Molecular biology and description of plasmids

KCNQ2 and KCNQ3 channel constructs were generated from human KCNQ2 and KCNQ3 clones (originally in the pTLN vector, provided by M. Taglialatela, University of Naples, Italy, and T. Jentsch, Max-Delbrück-Centrum für Molekulare Medizin, Germany), using the pcDNA3.1(−) plasmid (Invitrogen). Monomeric constructs were subcloned into pcDNA3.1(−) using NheI and EcoRI (KCNQ2) or XhoI and EcoRV (KCNQ3) restriction enzymes and verified by Sanger sequencing approaches (Genewiz or University of Alberta Applied Genomics Core). Concatenated KCNQ2 constructs were generated in pcDNA3.1(−) with the following design: NheI-COPY1(no stop)-XbaI-COPY2(no stop)-EcoRV-COPY3(no stop)-EcoRI-COPY4(no stop)-BamHI-GFP(STOP)-HindIII. No linkers were included in any of the protomers, apart from the restriction sites introduced for cloning. The sequence across the junctions were as follows (bold indicates nucleotides or amino acids introduced by the restriction sites): junction 1: 5′-GGGCCCAGGAAG*TCTAGA*GTGCAGAAGTCG-3′ (amino acid sequence: GPRK*SR*VQKS); junction 2: 5′-GGGCCCAGGAAG*GAT ATC*GTGCAGAAGTCG-3′ (amino acid sequence: GPRK*DI*VQKS); junction 3: 5′-GGGCCCAGGAAG*GAATTC*GTGCAGAAGTCG-3′ (amino acid sequence: GPRK*EF*VQKS); and junction 4 (KCNQ2 – GFP): 5′-GGGCCCAGGAAG*GGATCC*GTGAGCAAGGGC-3′ (amino acid sequence: GPRK*GS*VSKG).

The inclusion of a C-terminal GFP tag was helpful for the identification of positively transfected cells and also as an added confirmation that full-length tetrameric channels were synthesized in their entirety. Generation of mutant KCNQ2 plasmids (KCNQ2[F168L] and KCNQ2[A181P]) was performed with a two-step PCR method, described previously (Ho et al., 1989).

Cell culture and whole-cell patch-clamp recordings

HEK293 cells were cultured in 50-ml polystyrene tissue culture flasks (Falcon) in DMEM (Invitrogen) supplemented with 10% FBS and 1% penicillin-streptomycin. Cells were grown in an incubator at 5% CO_2 and 37°C. Cells were plated into six-well plates and cotransfected with plasmids encoding the channel of interest using jetPRIME DNA transfection reagent (Polyplus). For expression of monomeric subunits, plasmids were cotransfected with GFP to identify transfected cells, whereas the tetrameric con-

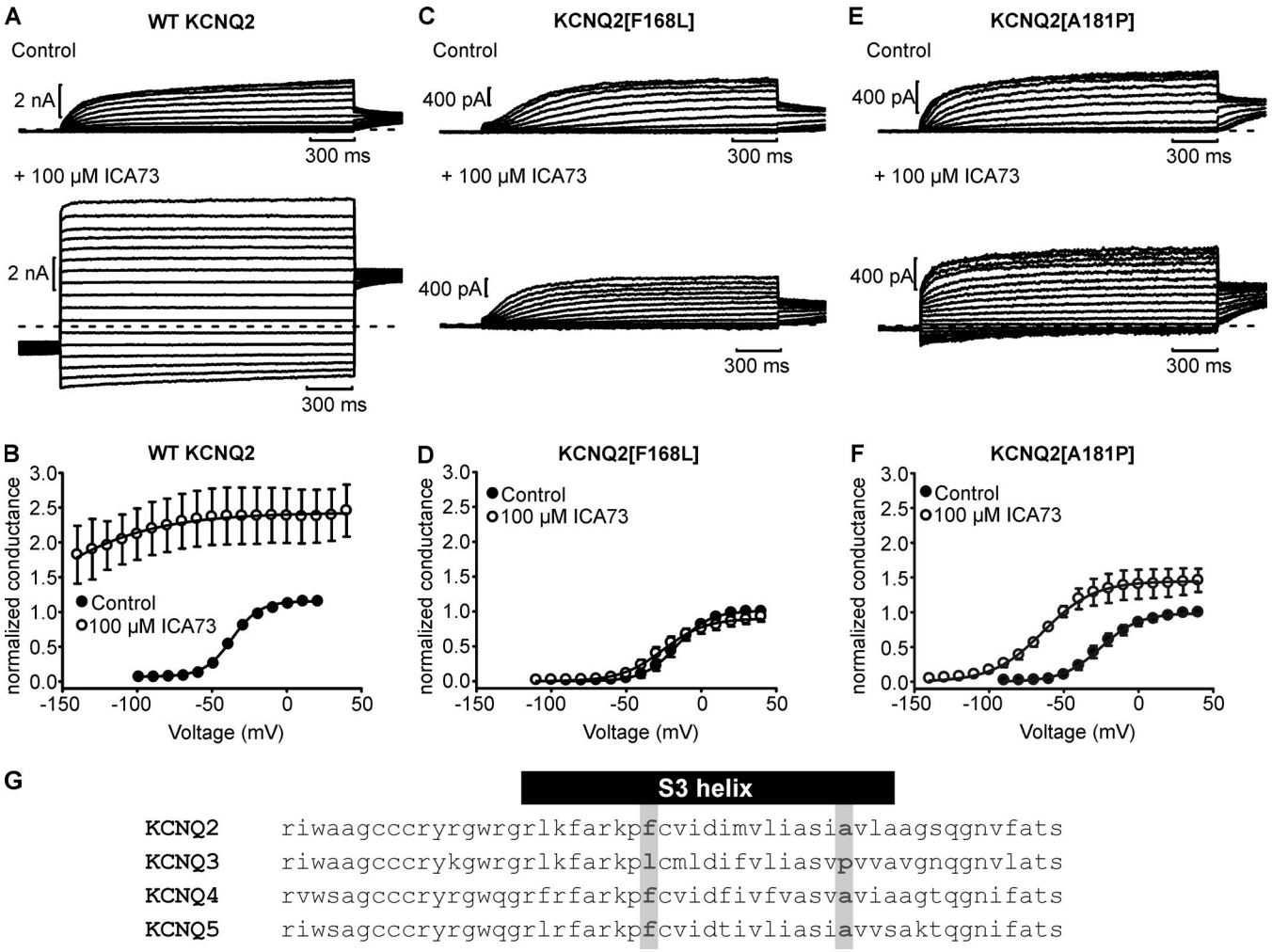

Figure 2. **Mutations in the VSD of KCNQ2 alter channel sensitivity to ICA73. (A, C, and E)** Exemplar patch-clamp records used to generate conductance–voltage relationships for WT KCNQ2, KCNQ2[F168L], and KCNQ2[A181P] channels, in control conditions (upper trace) and 100 µM ICA73. Channels were expressed in HEK293 cells, with a protocol identical to Fig. 1, but slightly altered voltage ranges to capture the full magnitude of the saturating drug effects. **(B, D, and F)** Tail current magnitude was normalized to the peak tail current observed in control conditions to generate conductance–voltage relationships. Gating parameters were WT KCNQ2 $V_{1/2}$ = −36 ± 4 mV, k = 13 ± 1 mV; KCNQ2[F168L] $V_{1/2}$ = −17 ± 4 mV, k = 10 ± 1 mV; and WT KCNQ2 $V_{1/2}$ = −24 ± 4 mV, k = 13 ± 2 mV. **(G)** Sequence alignment of the S3 segment and adjacent linkers of KCNQ2–5. Error bars are mean ± SEM.

structs had a fused C-terminal GFP tag that was used to identify transfected cells. After 48 h of incubation with transfection reagent, cells were split onto sterile glass coverslips at low density to allow recordings from individual cells, and electrophysiological experiments were conducted 1 d later.

Whole-cell patch-clamp recordings were performed using extracellular solution consisting of 135 mM NaCl, 5 mM KCl, 2.8 mM Na acetate, 1 mM $CaCl_2(2H_2O)$, 1 mM $MgCl_2(6H_2O)$, and 10 mM HEPES, with pH adjusted to 7.4. Intracellular solution contained 135 mM KCl, 5 mM EGTA, and 10 mM HEPES, with pH adjusted to 7.3. Glass pipette tips were manufactured using soda lime glass (Thermo Fisher Scientific) and had tip resistances of 1–3 MΩ in standard experimental solutions. Series resistance compensation of 75–85% was used in all recordings, and uncorrected series resistance did not exceed 4 MΩ. Recordings were filtered at 5 kHz and sampled at 10 kHz using an Axopatch-200B and a Digidata 1440A (Molecular Devices) controlled by pClamp 10 software (Molecular Devices). Chemicals were purchased from Thermo Fisher Scientific or Sigma-Aldrich. Experimental KCNQ channel opener compounds were purchased from Toronto Research Chemicals (retigabine) or Tocris (ICA73). They were stored as 100-mM stocks in DMSO and diluted to working concentrations in extracellular solution on each experimental day.

Two-electrode voltage-clamp solutions and recordings

For expression of monomeric KCNQ2 and KCNQ3 constructs in *Xenopus laevis* oocytes, complementary RNA was transcribed from the cDNA using the mMessage mMachine kit (Ambion). KCNQ2 and KCNQ3 in pTLN were linearized with MluI (KCNQ2) or HpaI (KCNQ3) and transcribed using the SP6 primer. Stage V–VI *X. laevis* oocytes were prepared as previously described (Shih et al., 1998) and injected with complementary RNA. Voltage-clamped potassium currents were recorded in a modified Ringer's solution (in mM): 116 NaCl, 2 KCl, 1 $MgCl_2$, 0.5 $CaCl_2$, and 5 HEPES, pH 7.4, using an OC-725C voltage clamp

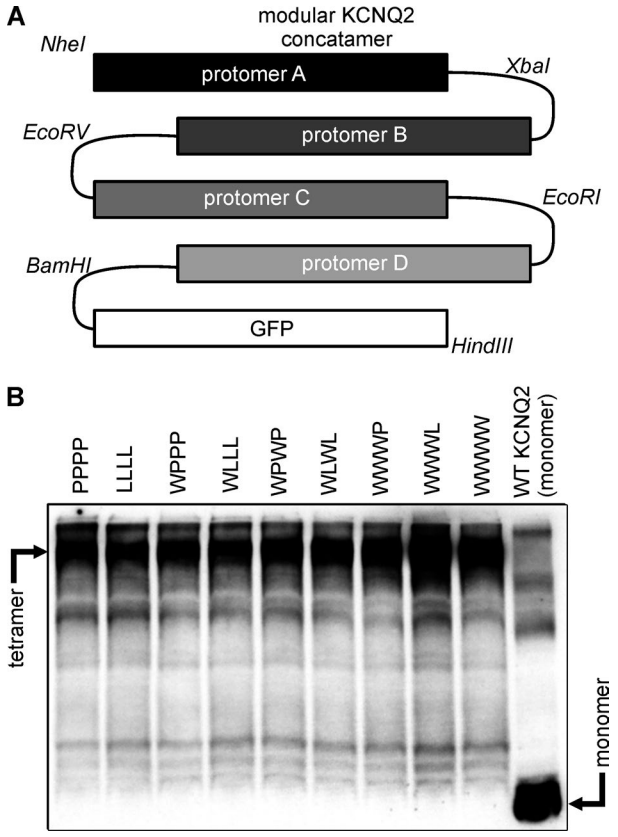

Figure 3. **Construction of a modular KCNQ2 concatemer. (A)** Schematic depiction of the arrangement of protomers and restriction enzyme sites used to interchange components of the tetrameric constructs. A GFP copy is appended to the C terminus to identify cells transfected with the full-length concatemer. **(B)** Western blot depicting lysates from HEK293 cells transfected with each concatemeric channel construct, as indicated (W = WT subunit, P = A181P subunit, L = F168L subunit). The concatemers predominantly run as a higher molecular weight band.

(Warner). Glass microelectrodes were backfilled with 3 M KCl and had resistances of 0.1–1 MΩ. Data were filtered at 5 kHz and digitized at 10 kHz using a Digidata 1440A controlled by pClamp 10 software.

Western blot protocol

Lysates from HEK cells transfected with KCNQ2 concatenated channel constructs were separated by gel electrophoresis on 7.0% SDS-PAGE gels and transferred to nitrocellulose blots using standard protocols. KCNQ2 protein was detected with a mouse monoclonal antibody (N26A/23, NeuroMAb) and HRP-conjugated rabbit anti-mouse secondary antibody (ABM) and visualized using ECL reagents and a FluorChem SP Gel Imager.

KCNQ channel molecular models

Molecular models of KCNQ2 and KCNQ3 were generated using the online SWISS-MODEL tool, based on the recent KCNQ1 cryo-EM structure (Sun and MacKinnon, 2017). These models are for illustration only and have not undergone refinement or development beyond the web-based homology modeling tool.

Data analysis

Voltage dependence of channel activation was fitted with a standard single-component Boltzmann equation of the form

$$G/G_{max} = \frac{1}{1 + e^{\frac{-(V-V_{1/2})}{k}}},$$

where $V_{1/2}$ is the voltage where channels exhibit half-maximal activation, and k is a slope factor reflecting the voltage range over which an e-fold change in open probability (P_o) is observed. Tail current deactivation kinetics were fitted with a single exponential equation in the form of $I(t) = I(0) \cdot e^{-t/\tau}$.

In channels with three or four ICA73-sensitive subunits, the drug-mediated gating shift was so large that we could not confidently fit their conductance–voltage relationships or tail current kinetics. Thus, where indicated, some conductance–voltage relationships in the presence of ICA73 have been fitted by a non-descriptive sigmoidal relationship, and we have not focused on specific gating parameters in these cases. Throughout the text and figures, data are presented as mean ± SEM.

Results

KCNQ2 homomers are affected more by VSD-targeted openers than KCNQ2/KCNQ3 heteromers

Previous studies have reported dramatic gating effects of a series of benzamide compounds including ICA-27243 and ICA73 on KCNQ2 channels, but with varying specificity for different KCNQ subtypes (Padilla et al., 2009; Wang et al., 2017). These compounds have some structural similarities to retigabine (Fig. 1, A and B), but their subtype specificity contrasts significantly from retigabine, which exhibits little specificity between KCNQ2–5. We have previously investigated ICA73 in detail, demonstrating a very strong hyperpolarizing shift and current potentiation in KCNQ2, with little effect in KCNQ3 (Wang et al., 2017). Because a significant portion of neuronal M-current is encoded by heteromeric KCNQ2/KCNQ3 channels (Hadley et al., 2003; Brown and Passmore, 2009), we also compared ICA73 effects on KCNQ2 versus heteromeric KCNQ2/KCNQ3 channels (Fig. 1, C and D). To collect responses in multiple drug concentrations, requiring lengthy protocols, data in Fig. 1 (C and D) was collected using the *X. laevis* expression system, whereas the remainder of the paper uses HEK293 cells to express various KCNQ2 concatenated tetrameric constructs (which did not express well in *X. laevis* oocytes).

KCNQ2/KCNQ3 channels exhibit a markedly attenuated response to ICA73. It is important to note that KCNQ2 deactivation is dramatically decelerated by ICA73, such that channels close extremely slowly even at very negative voltages (Fig. 1 E). This is a common feature of the benzamide class of KCNQ openers that target the VSD (Xiong et al., 2008; Blom et al., 2010; Gao et al., 2010; Wang et al., 2017). This effect is reflected in the conductance–voltage relationships presented (such as Fig. 1 C), as it was impractical to close channels completely in each interpulse interval. Thus, the protocol is described explicitly in the Fig. 1 legend, and it is important to note that the conductance–voltage relationship as shown does not necessarily represent an equilibrium result. The

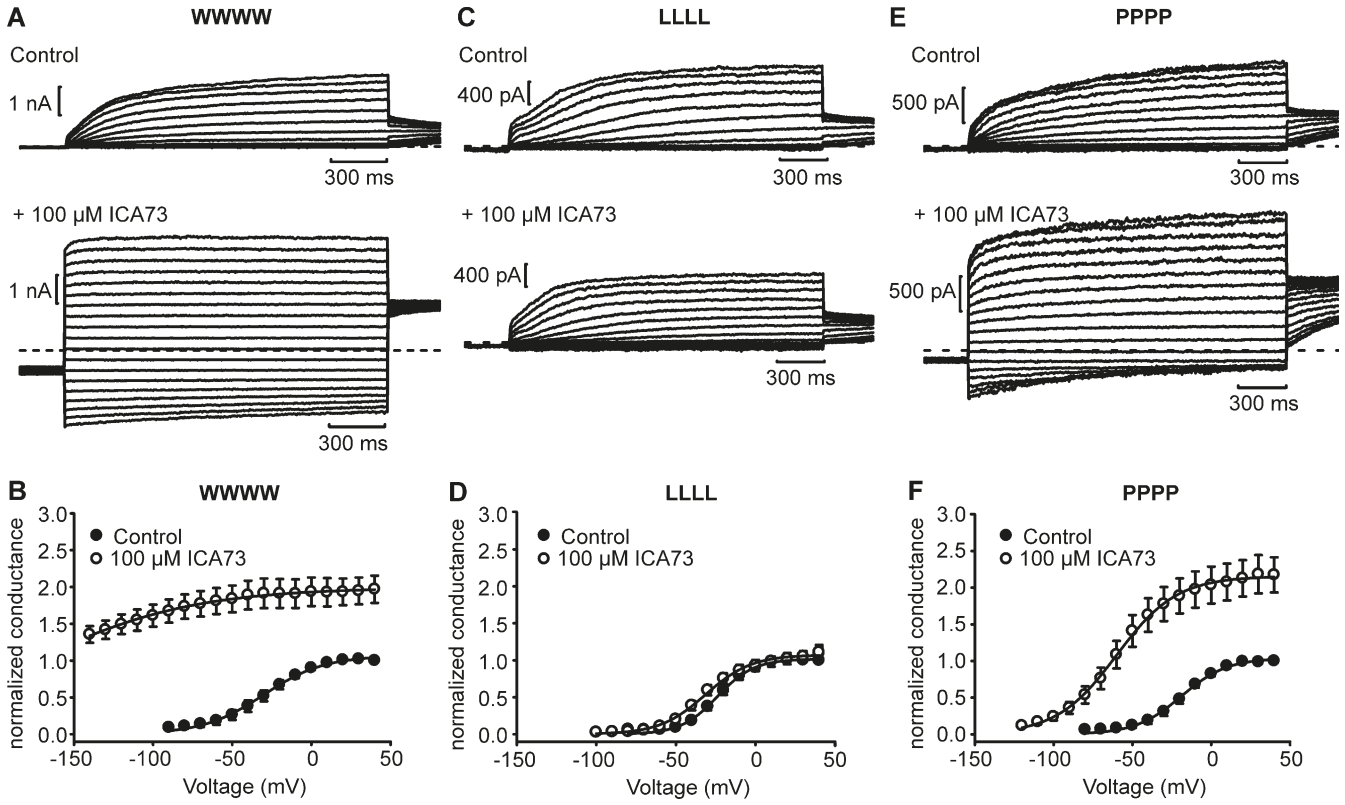

Figure 4. **Concatemeric channels recapitulate ICA73 sensitivity of VSD mutants. (A, C, and E)** Exemplar patch clamp records used to generate conductance–voltage relationships for WWWW (4 X WT KCNQ2), LLLL (4 X KCNQ2[F168L]), and PPPP (4 X KCNQ2[A181P]) channels in control conditions (upper trace) and 100 µM ICA73, as indicated, using an identical protocol as Figs. 1 and 2. **(B, D, and F)** Tail current magnitude was normalized to the peak tail current observed in control conditions to generate conductance–voltage relationships. Gating parameters were WWWW $V_{1/2}$ = −34 ± 5 mV, k = 16 ± 2 mV; LLLL $V_{1/2}$ = −24 ± 3 mV, k = 11 ± 2 mV; and PPPP $V_{1/2}$ = −23 ± 3 mV, k = 12 ± 1 mV. Error bars are mean ± SEM.

dramatic effects of ICA73 on KCNQ2 versus KCNQ2/3 deactivation are highlighted in Fig. 1 E, illustrating that the heteromeric channels are able to close much more rapidly in the presence of ICA73.

Mutations in the KCNQ2 voltage sensor weaken the effects of ICA73

We previously demonstrated that ICA73 effects could be attenuated or abolished by mutations identified by scanning sequence differences between the VSD of KCNQ2 and KCNQ3, and that this accounted for ICA73 subtype specificity for KCNQ2 over KCNQ3 (Wang et al., 2017). We identified KCNQ2 amino acids F168 (S2–S3 linker) and A181 (S3) in the voltage-sensing module as important determinants of ICA73 sensitivity. Data in Fig. 2 recapitulate the finding that F168L and A181P mutations in KCNQ2 attenuate ICA73-mediated effects. Up to the limits of solubility of ICA73 (~100 µM), KCNQ2[F168L] channels appear to be completely insensitive to ICA73, with no apparent gating shift and minimal current potentiation (Fig. 2, C and D). The KCNQ2[A181P] mutant exhibits weakened sensitivity to ICA73, with a modest gating shift in 100 µM ICA73 (Fig. 2, E and F) and some current potentiation. Our previous study tested ICA73 concentrations as high as 30 µM, which caused very little voltage shift, whereas the current dataset in a higher concentration of ICA73 reveals both a modest voltage shift and some potentiation. Unfortunately, we cannot absolutely distinguish whether this is caused by partial agonism versus weaker potency of ICA73 toward KCNQ2[A181P] mutants, because we cannot apply concentrations much higher than 100 µM. The details of the binding site for ICA73 and other benzamides have not been studied with nearly the same detail as retigabine, and so it is not clear whether amino acids A181 and F168 residues are directly involved in binding, alter the structure of the binding site, or alter coupling of the voltage sensor and pore domains (Wang et al., 2017).

We have highlighted KCNQ2 F168 and A181 in a sequence alignment of the S3 helix region and neighboring linkers of KCNQ2–5 channels (Fig. 2 G), illustrating their high homology in this region. A181 has not been examined in detail outside the scope of our prior investigation of ICA73 sensitivity (Wang et al., 2017). Residue F168 has been previously mutated as part of a strategy to modulate stability of the voltage sensor resting state (Miceli et al., 2013), but there is not a well supported mechanistic explanation for its powerful suppression of ICA73 sensitivity. Other side chains in the voltage sensor have also been reported to alter sensitivity to various voltage sensor–targeted compounds, including Y127, E130, and R207 (Li et al., 2013; Peretz et al., 2010), although again, a mechanistic understanding of voltage sensor–targeted KCNQ openers has not been well established.

Concatenated KCNQ2 recapitulates properties of homomeric channels

We developed a modular concatenated KCNQ2 tetrameric construct with a C-terminal GFP tag (Fig. 3 A). This construct allowed

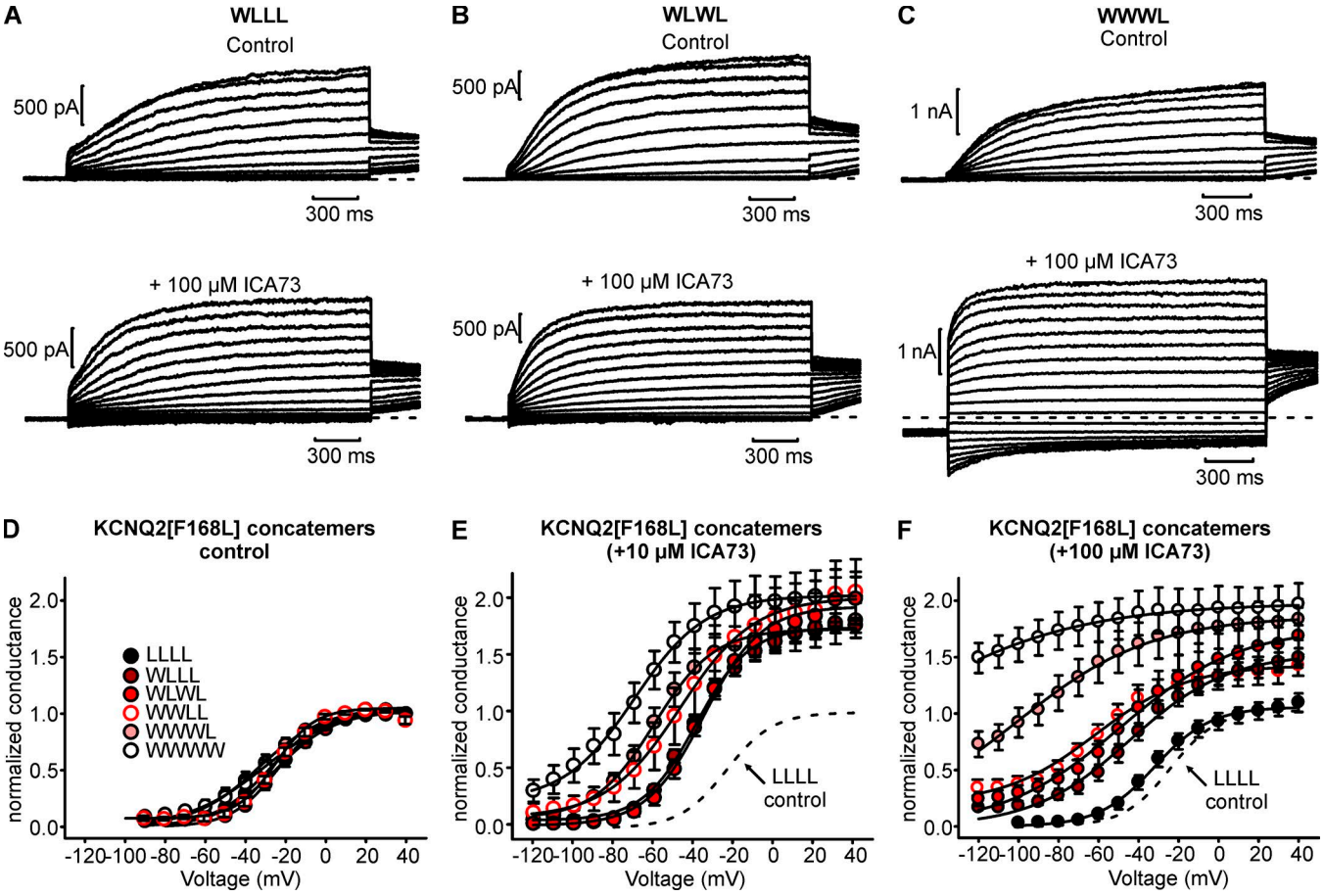

Figure 5. **ICA73 sensitivity depends on the number of drug-sensitive subunits. (A–C)** Exemplar patch clamp records used to generate conductance–voltage relationships for WLLL (1 X WT KCNQ2 + 3 X KCNQ2[F168L]), WLWL (2 X WT KCNQ2 + 2 X KCNQ2[F168L]), and WWWL (3 X WT KCNQ2 + 1 X KCNQ2[F168L]) channels, in control conditions (upper trace) and 100 μM ICA73, as indicated, using an identical protocol to Figs. 1 and 2. **(D–F)** Tail current magnitude was normalized to the peak tail current observed in control conditions to generate conductance–voltage relationships. In 100 μM ICA73 F, a clear progression in ICA73 effect is observed with increasing numbers of ICA73-sensitive subunits. In 10 μM ICA73 E, gating parameters for the various concatemers were WWWW $V_{1/2}$ = −71 ± 6 mV, k = 17 ± 2 mV; WWWL $V_{1/2}$ = −60 ± 4 mV, k = 15 ± 2 mV; WWLL $V_{1/2}$ = −50 ± 5 mV, k = 18 ± 6 mV; WLWL $V_{1/2}$ = −40 ± 2 mV, k = 13 ± 2 mV; and WLLL $V_{1/2}$ = −40 ± 2 mV, k = 14 ± 1 mV. LLLL control (dashed line in E and F is the fit of the corresponding data in panel D, for comparison). In control conditions, gating parameters were WWWW $V_{1/2}$ = −20 ± 3 mV, k = 8.4 ± 0.5 mV; WWWL $V_{1/2}$ = −23 ± 3 mV, k = 8.2 ± 0.5 mV; WWLL $V_{1/2}$ = −19 ± 3 mV, k = 8.7 ± 0.6 mV; WLWL $V_{1/2}$ = −14 ± 3 mV, k = 9.8 ± 0.9 mV; and WLLL $V_{1/2}$ = −22 ± 2 mV, k = 7.7 ± 0.5 mV. The number of KCNQ2[F168L] subunits in the tetramer alters the response to ICA73. Error bars are mean ± SEM.

us to swap individual protomers using restriction digests and to sequence significant regions of inserted protomers to confirm the presence of desired mutations. We generated and expressed a variety of tetramers with varying numbers of WT (W), F168L (L), or A181P (P) subunits. During patch clamp experiments, the C-terminal GFP fusion enabled identification of successfully transfected cells and increased our confidence that full-length tetrameric channels were being translated. We also confirmed translation of full-length KCNQ2 tetrameric constructs using Western blots (Fig. 3 B), demonstrating that the predominant protein recognized by the KCNQ2 antibody corresponded to the full-length concatenated channel construct.

Control concatenated channels exhibited properties similar to homomeric channels (Fig. 4). The WWWW (4 × WT KCNQ2) tetramer was strongly shifted and potentiated by 100 μM ICA73 (Fig. 4, A and B), the LLLL tetramer (4 × KCNQ2[F168L]) was completely insensitive to ICA73 (Fig. 4, C and D), and the PPPP tetramer (4 × KCNQ2[A181P]) exhibited some current potentiation but an attenuated ICA73-mediated gating shift (Fig. 4, E and F). In these experiments, the degree of potentiation of PPPP channels was more pronounced than observed for monomeric KCNQ2[A181P] channels (Fig. 2, E and F). However, we have found the degree of current potentiation to be quite variable from cell to cell and between experimental days, and we have not investigated the effects of ICA73 on current potentiation in significant detail (this is discussed later when characterizing various A181 concatemers). As mentioned previously, it is important to bear in mind that the extremely slow closure of WWWW channels in the presence of ICA73 causes the properties of the conductance–voltage relationship to depend on the pulse history and frequency, because it is challenging to achieve complete channel closure between sweeps in the presence of ICA73. Nevertheless, the gating phenotype is consistent between homomeric constructs and the WWWW, LLLL, and PPPP concatenated channels (Figs. 2 and 4).

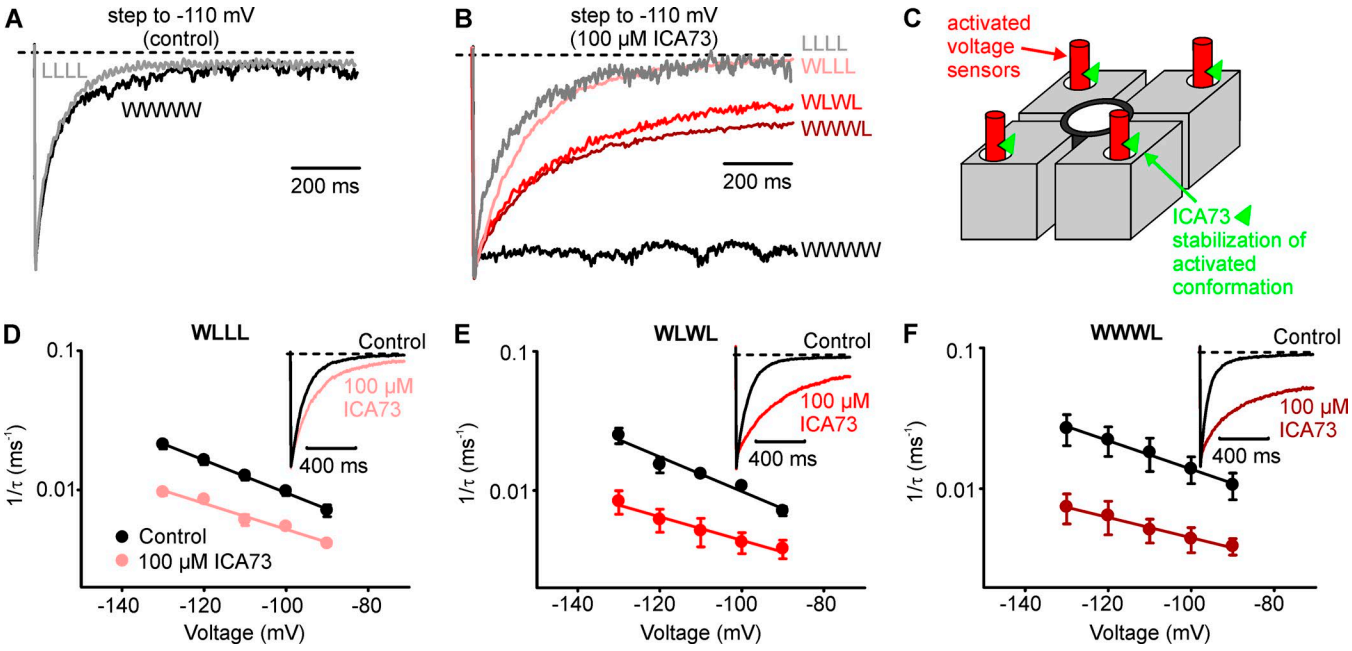

Figure 6. **ICA73 alters the extent of KCNQ2 channel closure and is affected by the number of drug-sensitive subunits. (A and B)** Exemplar patch-clamp records depicting channel deactivation for indicated concatemeric constructs, in control conditions A and 100 µM ICA73 B, elicited by a step to −110 mV after an initial depolarization to +20 mV. The presence of one or more drug-insensitive subunits allows for a rapid component of channel deactivation, but to a different extent. **(C)** Cartoon depiction of the hypothesized action of ICA73, via stabilization of the active conformation of the voltage sensor. **(D–F)** Time constants of tail current decay were measured for each concatemer over a range of test voltages (after a depolarization to +20 mV) and fitted with a single exponential decay equation for 1 s after repolarization to the test voltage. Error bars are mean ± SEM.

Multiple voltage sensor sites are required for ICA73 effects

We tested a series of concatemers with varying numbers of WT KCNQ2 and ICA73-insensitive KCNQ2[F168L] subunits for their response to 10 and 100 µM ICA73 (Fig. 5, A–C). Changing the ratio of ICA73-sensitive and -insensitive subunits had no remarkable effects on the voltage dependence of channel gating in control conditions (Fig. 5 D). However, the ICA73 response depended strongly on the number of ICA73-sensitive subunits (Fig. 5, E and F). The presence of one (WLLL) or two (WLWL) ICA73-sensitive subunits led to a clearly attenuated response to ICA73 (Fig. 5, A, B, E, and F). We observed a small difference in the response of the WWLL versus WLWL tetramers (alternating vs. side-by-side orientation of the mutant and WT protomers) in 10 µM ICA73 (Fig. 5 E), but this was less obvious in 100 µM ICA73 (Fig. 5 F). Even the presence of three WT KCNQ2 subunits was not sufficient to generate the full response observed in WT KCNQ2 or the WWWW tetramer (Fig. 5, C, E, and F).

The importance of a full complement of ICA73-sensitive subunits is most apparent when examining tail current decay (Fig. 6). Although the subunit stoichiometry had little effect on deactivation in the absence of ICA73 (Fig. 6 A), concatemers differed markedly in the presence of the drug. As mentioned earlier, deactivation of WT or WWWW channels is extremely slow in the presence of saturating concentrations of ICA73 (Fig. 6 B, black), and given that mutations that alter ICA73 sensitivity are clustered in the VSD, we infer that this slower channel closure is caused by drug-mediated stabilization of the activated VSD conformation (Fig. 6 C). In contrast, incorporation of one or more KCNQ2[F168L] subunits resulted in significant current decay upon repolarization (Fig. 6 B). The presence of varying numbers of F168L subunits did not dramatically affect the kinetics of tail current decay (Fig. 6, D–F); however, there were notable effects on the relative magnitude of the rapid component of current decay (Fig. 6 B). For example, in WWWL or WLWL channels, there was a clear persistent slow component of current decay, whereas tail currents in WLLL or LLLL channels decayed more completely within 1 s of repolarization of the membrane voltage (Fig. 6 B). It is clear that the dramatic ICA73-mediated deceleration of KCNQ2 closure (Figs. 1 E and 6 B) strictly requires four ICA73-sensitive subunits.

KCNQ2[A181P] mutant channels have an attenuated ICA73-mediated shift in voltage-dependent gating but preserved current potentiation (Figs. 2 F and 4 F). Similar to our approach with F168L concatemers, we tested a series of channels with different numbers of A181P subunits (Fig. 7, A–C). In this instance, the retained sensitivity to current potentiation led to variability in the degree of current potentiation between cells and experimental days. Because of this significant variability, we normalized the conductance–voltage relationships to more clearly illustrate the effects on activation gating in tetramers with different numbers of ICA73-sensitive subunits (Fig. 7, D and E). As observed for the F168L tetramers, there was very little drug-mediated gating shift with one or two WT KCNQ2 subunits present, and four WT subunits appeared to be essential for the full gating effect of ICA73 (Fig. 7 E). An illustration of the conserved potentiation between WT KCNQ2 and A181P mutants is presented in Fig. 7 F. Overall, the WWWW (2.0 ± 0.3-fold) and PPPP tetramers (2.0 ± 0.2-fold) exhibited a similar average potentiation, and in

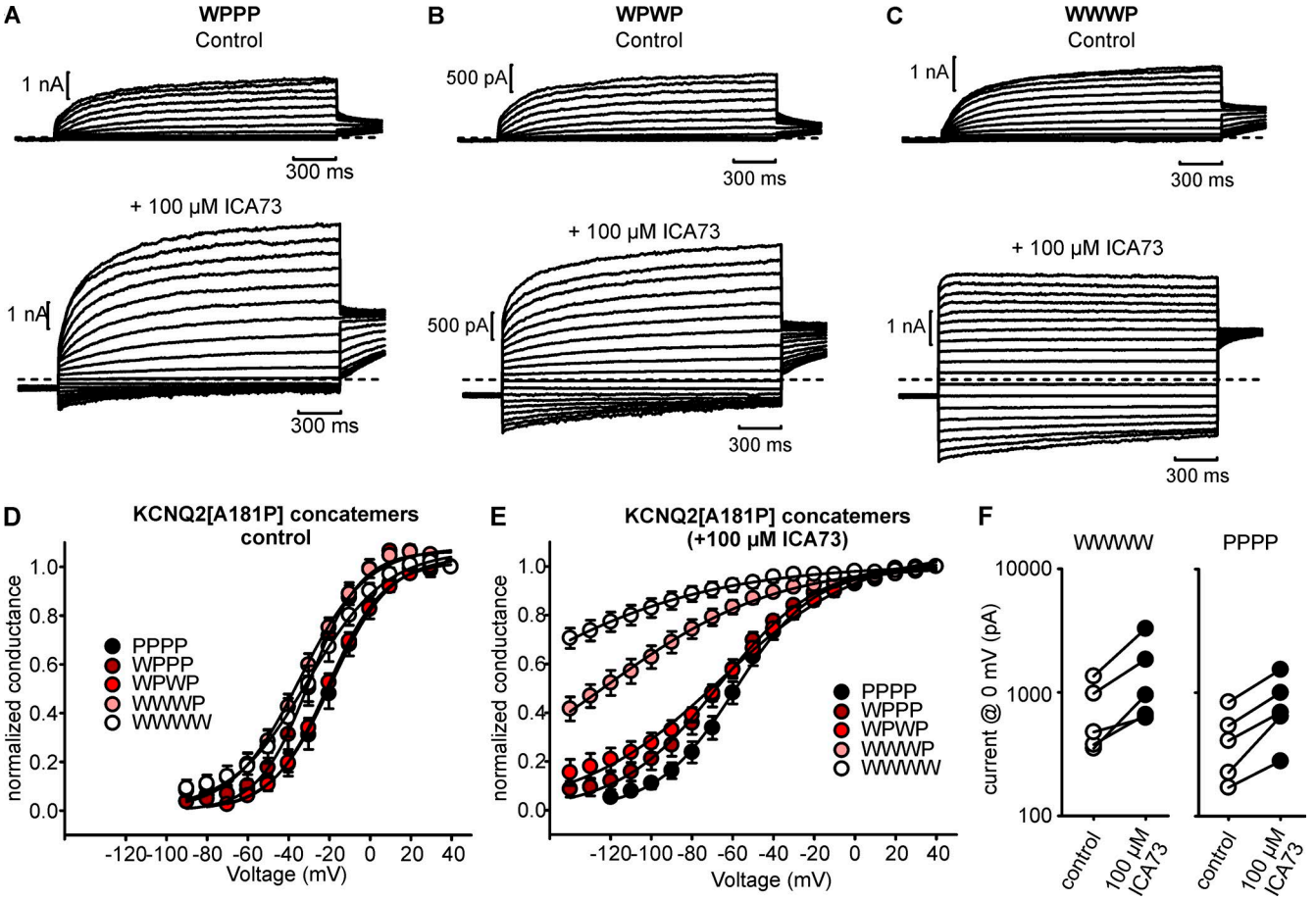

Figure 7. **The number of KCNQ2[A181P] subunits also influences ICA73 sensitivity. (A–C)** Exemplar patch clamp records used to generate conductance–voltage relationships for WPPP (1 X WT KCNQ2 + 3 X KCNQ2[A181P]), WPWP (2 X WT KCNQ2 + 2 X KCNQ2[A181P]), and WWWP (3 X WT KCNQ2 + 1 X KCNQ2[A181P]) channels, in control conditions (upper trace) and 100 µM ICA73, as indicated, using an identical protocol to Figs. 1 and 2. Unlike previous figures, tail current magnitude was normalized to the peak tail current for each respective recording, because KCNQ2[A181P] mutants retain partial sensitivity to ICA73, leading to highly variable levels of current potentiation between cells. **(D and E)** Normalized conductance–voltage relationships for control conditions and in 100 µM ICA73. The number of KCNQ2[A181P] subunits in the tetramer alters the response to ICA73. **(F)** ICA73-mediated potentiation of currents on a cell-by-cell basis for WWWW or PPPP concatenated channels. Error bars are mean ± SEM.

paired experiments including a control and drug wash-on, some amount of potentiation was consistently observed. Data from individual cells for all the tetramers tested in this study show that potentiation varied from 1.3- to 3.2-fold, and there was no consistent pattern of the extent of potentiation observed in different constructs.

Discussion

We investigated the subunit composition requirement underlying the effects of the neuronal KCNQ channel activator ICA73. Previous research has suggested that ICA73 and related compounds differ in their mechanism of action relative to the better-characterized KCNQ opener retigabine, despite superficial structural similarities between these molecules (Padilla et al., 2009; Li et al., 2013; Wang et al., 2017). Early experiments using various KCNQ2:KCNQ5 chimeras demonstrated that alterations of the VSD could strongly attenuate effects of the related compound ICA27243, although mutations of the conserved pore Trp that is required for retigabine sensitivity did not alter ICA27243 effects (Padilla et al., 2009). A subsequent mutation-based analysis of the KCNQ2 voltage sensor (motivated by comparisons with the ICA73-insensitive KCNQ3 subtype) led to the identification of KCNQ2 VSD side chains F168 (S2–S3 linker) and A181 (S3) as important determinants of ICA73 sensitivity (Wang et al., 2017).

Exploration of detailed aspects of the binding site for ICA73 and other voltage sensor–targeted Kv7 activators is ongoing, although our understanding lags behind the more complete description of retigabine binding that has been attained. Based on the available cryo-EM KCNQ1 structure, the estimated α-carbon distance between A181 and F168 acid positions is ∼18 Å, while the end-to-end length of ICA73 is ∼12 Å, so it is unclear whether both amino acids contribute to the same binding site (Sun and MacKinnon, 2017). In addition, effects of ICA73 on current potentiation versus voltage-dependent activation appear to be distinctly regulated, as the A181P mutation perturbs the shift in voltage dependence but preserves ICA73-mediated potentiation (Wang et al., 2017). A181, F168, and other amino acids (E130, Y127, and R207) proposed to influence drug actions in the VSD will require further study to understand their relative contributions to

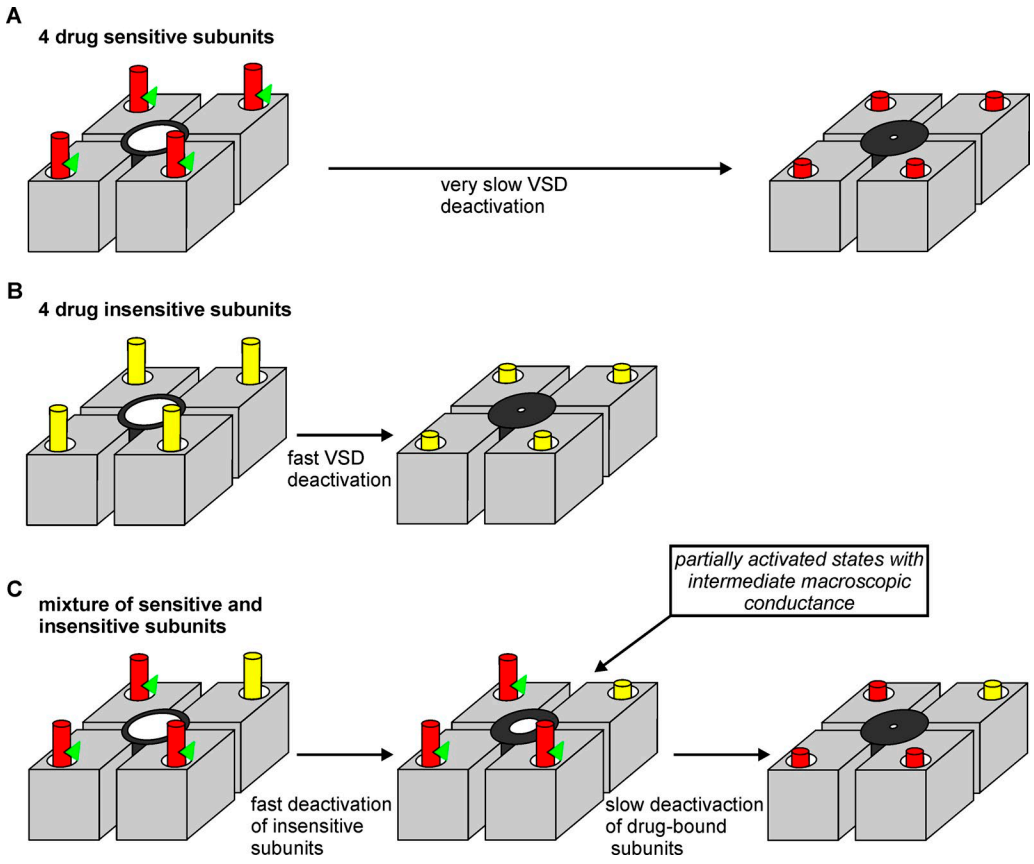

Figure 8. **Model of the mechanism of action of voltage sensor–targeted KCNQ2 channel openers.** This cartoon depicts voltage sensors in the activated or resting conformations in various arrangements of drug-sensitive (red) and -insensitive (yellow) subunits. We speculate that ICA73 and similar compounds act by stabilizing the activated conformation of the VSD (depicted as a green "doorstop" propping up the activated voltage sensor). **(A)** When a channel is composed of four drug-sensitive subunits, drug unbinding from each subunit markedly delays channel closure. **(B)** When a channel is composed of four drug-insensitive subunits (e.g., KCNQ2[F168L]), the VSDs can deactivate unimpeded, leading to rapid deactivation in the presence of the drug. **(C)** When a channel is composed of a mixture of drug-sensitive and -insensitive subunits, we speculate that rapid deactivation of drug-insensitive subunits leads to an intermediate open state resulting in an intermediate macroscopic conductance (illustrated as partially closed central pore), followed by further slow channel closure resulting from slow deactivation of drug-sensitive subunits. Note that we cannot distinguish whether this would be caused by an intermediate single channel conductance, an intermediate open probability, or a combination of both.

drug binding, coupling, or voltage sensor conformation (Peretz et al., 2010; Li et al., 2013). For the purposes of this study, the A181P and F168L mutations were used in parallel to alter the number of drug-sensitive subunits and investigate the stoichiometry of ICA73 actions, and they generated consistent results.

KCNQ3* concatemers (Yau et al., 2018) illustrate that a single retigabine-sensitive subunit is sufficient for a near-maximal retigabine effect. In contrast, the series of F168L and A181P concatemers reported here demonstrate a different stoichiometric requirement for voltage sensor–targeted drugs such as ICA73, as a full complement of four ICA73-sensitive KCNQ2 subunits is required for the full ICA73-mediated effect. This is consistent with the marked attenuation of ICA73 effects on heteromeric channels comprising KCNQ2 (ICA73-sensitive) and KCNQ3 (ICA73-insensitive; Fig. 1). The incorporation of even a single ICA73-insensitive subunit interferes with the effectiveness of ICA73 on channel closure (Fig. 6 B). Also, the clear progression of ICA73 effectiveness in the sets of generated concatemers is a good indication that the concatemers typically assemble correctly (McCormack et al., 1992; Sack et al., 2008). Given the varied subunit composition of KCNQ channels in the brain and other organs, this finding reinforces the importance of considering subtype specificity and stoichiometry of drug effects when screening newly developed compounds (Brown and Passmore, 2009). In the context of targeting neuronal KCNQ potassium channels, it is important to distinguish the effects of drugs such as ICA73 on WT KCNQ2 channels from those on KCNQ2/KCNQ3 heteromeric channels, which are more likely to be present in native tissue (Miceli et al., 2008; Barrese et al., 2018). ICA73 has remarkable effects on homomeric KCNQ2 channels, which it appears to essentially lock in the open state, requiring many seconds for complete channel closure, even at the most hyperpolarized voltages tested (Fig. 1 E). ICA73 effects on KCNQ2/KCNQ3 heteromers are attenuated quite markedly, a reflection of the stoichiometric requirement for a full complement of ICA73-sensitive subunits demonstrated in this study. We have shown here that the presence of one or more ICA73-insensitive KCNQ3 subunits would markedly attenuate channel sensitivity to ICA73 (Figs. 5, 6, and 7).

Given the sensitivity of ICA73 and related compounds to mutations in the VSD, but not the pore domain, a preliminary

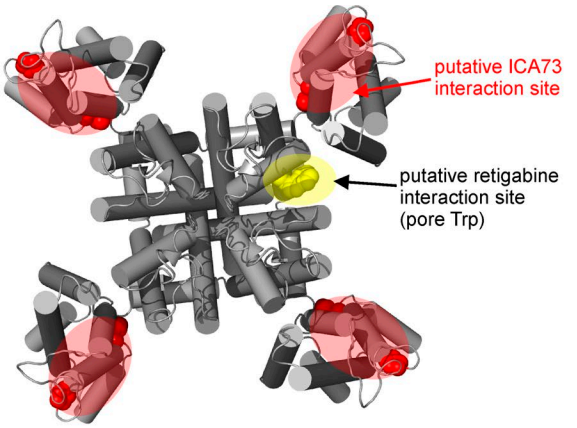

	Pore-targeted drugs	VSD-targeted drugs
location of putative binding site	pore	voltage sensor
disrupting mutations	Trp 236 (KCNQ2), Trp 265 (KCNQ3)	Phe168, Ala181 (KCNQ2)
requirement for polar H-bond acceptor	YES	NO
drug-sensitive subunits required for full effect	~1	4
subtype specificity	NO	YES

Figure 9. **Contrasting mechanism and stoichiometry of pore- and voltage sensor–targeted KCNQ openers.** Top: Top view of a model KCNQ channel based on the recent KCNQ1 cryo-EM structure (PDB accession no. 5VMS). The location of mutations that alter ICA73 sensitivity (A181, F168) are highlighted by the red oval in each voltage sensor, depicting the requirement of four binding events for the full drug effect. The location of residues essential for retigabine binding (W236) are highlighted in yellow in only one subunit, depicting the requirement for only one binding event (Yau et al., 2018). Bottom: Table summarizing critical differences in mechanism, stoichiometry, putative binding site, and subunit sensitivity to voltage sensor– and pore-targeted KCNQ openers.

model for their mode of action is immobilization of an activated conformation of the VSD (Fig. 6 C and 8 A). The related KCNQ1 subtype is believed to occupy multiple open states depending on the number of activated VSDs—not all VSDs need to be activated for the pore to open (Meisel et al., 2012; Osteen et al., 2012). A similar allosteric mechanism in KCNQ2 would account for the observed behavior of channels with one or more ICA73-insensitive subunits. That is, upon hyperpolarization, insensitive VSDs would deactivate quickly (Fig. 8 B), and in channels with mixed ICA73-sensitive and -insensitive subunits, this would result in current relaxation to an intermediate open state with a fraction of activated voltage sensors, followed by slower deactivation of drug-occupied VSDs (Fig. 8 C). A close analogy would be the persistent current observed at negative voltages in heteromers of WT KCNQ1 and the constitutively active KCNQ1 voltage-sensor mutant R213C (Osteen et al., 2012). Similar to what we observe with intermediate numbers of ICA73-sensitive subunits (Fig. 6), the heteromeric KCNQ1:R213C channel is thought to deactivate to a partially activated state (with two activated voltage sensors in a 1:1 KCNQ1:R213C ratio) leading to a persistent intermediate conductance even at very negative voltages. In the case of ICA73 binding to KCNQ2 channels, the analogy to this persistent current would be the slow component of current decay as drug-bound ICA73-sensitive subunits slowly deactivate (Fig. 6, B and C).

Although there has not yet been a direct investigation of the relationship between VSD and pore activation in KCNQ2, some findings suggest an allosteric model of activation. Importantly, KCNQ2/3 heteromeric channels exhibit variable open probability depending on the number of PIP2-sensitive subunits (Telezhkin et al., 2012), although unlike KCNQ1, there has not been a demonstration of subconductance states linked to intermediate numbers of activated VSDs (Werry et al., 2013; Hou et al., 2017). They also exhibit a similar requirement for PIP2 to couple the VSD and pore (Zaydman et al., 2013; Zaydman and Cui, 2014; Kim et al., 2017). A variety of experimental approaches have been used to investigate allosteric activation models of KCNQ1, and we hope to extend our study in the future to include some of these approaches in combination with the unique pharmacology of KCNQ2 to deduce principles of pharmacology and voltage-dependent activation of the neuronal M-current.

This study should be considered in the context of Yau et al. (2018) describing functional stoichiometry of retigabine action, in which we demonstrated that near-maximal retigabine effects can be achieved with a single retigabine-sensitive subunit. This marked difference in stoichiometric requirements supports the notion of distinct mechanisms of action and binding sites for pore- versus VSD-targeted KCNQ channel openers, summarized in Fig. 9. Using a molecular model based on the recent KCNQ1 structure, we have highlighted the approximate location of A181 and F168, which have been shown to influence ICA73 sensitivity (red), and the W236 position that is essential for retigabine sensitivity (yellow). Overall, pore-delimited openers such as retigabine and VSD-targeted openers such as ICA73 differ in their subtype specificity, stoichiometry, and putative location of binding. Four voltage sensors have been highlighted to contrast the requirement of four ICA73-sensitive subunits versus a single retigabine-sensitive subunit. In addition, several mutations have been identified that uniquely affect one drug class, but not the other (such as KCNQ2[F168L] and KCNQ2[A181P], which perturb ICA73 actions but not retigabine, whereas KCNQ2[W236L] abolishes retigabine sensitivity but retains sensitivity to ICA73; Wang et al., 2017). One other important detail is that our previous work highlighted the importance of a polar H-bond acceptor for actions on the pore-delimited retigabine site in KCNQ3 (Kim et al., 2015). This property is clearly not required for action at the VSD site, as drugs like ICA73 have very weak polarity relative to retigabine (and correspondingly weak effects at the retigabine site in KCNQ3), but very powerful effects at the VSD site in KCNQ2 (Gao et al., 2010; Li et al., 2013; Kim et al., 2015; Wang et al., 2017).

Overall, our investigation of functional stoichiometry of diverse KCNQ activator compounds provides important contrasting descriptions of the underlying mechanisms of action of retigabine (pore-targeted) and ICA73 (VSD-targeted). We are hopeful that continued improvement of our understanding of

the variety of ways that drugs can promote activation of KCNQ channels will contribute to the ongoing development of this interesting drug class.

Acknowledgments

This study was funded by Canadian Institutes of Health Research operating grant MOP 142482. Caroline K. Wang was supported by a Canadian Institutes of Health Research CGS-M graduate award. S.A. Pless was supported by a Lundbeck Foundation Fellowship (R139-2012-12390). Harley T. Kurata is supported by a Canadian Institutes of Health Research New Investigator Award and the Alberta Diabetes Institute.

The authors declare no competing financial interests.

Author contributions: A. Wang, M. Yau, S. Pless, and H. Kurata conceived the project and designed experiments. A. Wan, M. Yau, C. Wang, N. Sharmin, R. Yang, and H. Kurata performed experiments and analyzed data. A. Wang and H. Kurata wrote the manuscript. All authors contributed to editing and revisions of the final version of the manuscript.

Kenton J. Swartz served as editor.

Submitted: 26 January 2018
Accepted: 6 August 2018

References

Barrese, V., J.B. Stott, and I.A. Greenwood. 2018. KCNQ-Encoded Potassium Channels as Therapeutic Targets. *Annu. Rev. Pharmacol. Toxicol.* 58:625–648. https://doi.org/10.1146/annurev-pharmtox-010617-052912

Bentzen, B.H., N. Schmitt, K. Calloe, W. Dalby Brown, M. Grunnet, and S.P. Olesen. 2006. The acrylamide (S)-1 differentially affects Kv7 (KCNQ) potassium channels. *Neuropharmacology.* 51:1068–1077. https://doi.org/10.1016/j.neuropharm.2006.07.001

Blom, S.M., N. Schmitt, and H.S. Jensen. 2010. Differential effects of ICA-27243 on cloned K(V)7 channels. *Pharmacology.* 86:174–181. https://doi.org/10.1159/000317525

Brodie, M.J., H. Lerche, A. Gil-Nagel, C. Elger, S. Hall, P. Shin, V. Nohria, and H. Mansbach. RESTORE 2 Study Group. 2010. Efficacy and safety of adjunctive ezogabine (retigabine) in refractory partial epilepsy. *Neurology.* 75:1817–1824. https://doi.org/10.1212/WNL.0b013e3181fd6170

Brown, D.A., and G.M. Passmore. 2009. Neural KCNQ (Kv7) channels. *Br. J. Pharmacol.* 156:1185–1195. https://doi.org/10.1111/j.1476-5381.2009.00111.x

Delmas, P., and D.A. Brown. 2005. Pathways modulating neural KCNQ/M (Kv7) potassium channels. *Nat. Rev. Neurosci.* 6:850–862. https://doi.org/10.1038/nrn1785

Gao, Z., T. Zhang, M. Wu, Q. Xiong, H. Sun, Y. Zhang, L. Zu, W. Wang, and M. Li. 2010. Isoform-specific prolongation of Kv7 (KCNQ) potassium channel opening mediated by new molecular determinants for drug-channel interactions. *J. Biol. Chem.* 285:28322–28332. https://doi.org/10.1074/jbc.M110.116392

Hadley, J.K., G.M. Passmore, L. Tatulian, M. Al-Qatari, F. Ye, A.D. Wickenden, and D.A. Brown. 2003. Stoichiometry of expressed KCNQ2/KCNQ3 potassium channels and subunit composition of native ganglionic M channels deduced from block by tetraethylammonium. *J. Neurosci.* 23:5012–5019. https://doi.org/10.1523/JNEUROSCI.23-12-05012.2003

Ho, S.N., H.D. Hunt, R.M. Horton, J.K. Pullen, and L.R. Pease. 1989. Site-directed mutagenesis by overlap extension using the polymerase chain reaction. *Gene.* 77:51–59. https://doi.org/10.1016/0378-1119(89)90358-2

Hou, P., J. Eldstrom, J. Shi, L. Zhong, K. McFarland, Y. Gao, D. Fedida, and J. Cui. 2017. Inactivation of KCNQ1 potassium channels reveals dynamic coupling between voltage sensing and pore opening. *Nat. Commun.* 8:1730. https://doi.org/10.1038/s41467-017-01911-8

Kim, R.Y., M.C. Yau, J.D. Galpin, G. Seebohm, C.A. Ahern, S.A. Pless, and H.T. Kurata. 2015. Atomic basis for therapeutic activation of neuronal potassium channels. *Nat. Commun.* 6:8116. https://doi.org/10.1038/ncomms9116

Kim, R.Y., S.A. Pless, and H.T. Kurata. 2017. PIP2 mediates functional coupling and pharmacology of neuronal KCNQ channels. *Proc. Natl. Acad. Sci. USA.* 114:E9702–E9711. https://doi.org/10.1073/pnas.1705802114

Lange, W., J. Geissendörfer, A. Schenzer, J. Grötzinger, G. Seebohm, T. Friedrich, and M. Schwake. 2009. Refinement of the binding site and mode of action of the anticonvulsant Retigabine on KCNQ K+ channels. *Mol. Pharmacol.* 75:272–280. https://doi.org/10.1124/mol.108.052282

Li, P., Z. Chen, H. Xu, H. Sun, H. Li, H. Liu, H. Yang, Z. Gao, H. Jiang, and M. Li. 2013. The gating charge pathway of an epilepsy-associated potassium channel accommodates chemical ligands. *Cell Res.* 23:1106–1118. https://doi.org/10.1038/cr.2013.82

Mackie, A.R., and K.L. Byron. 2008. Cardiovascular KCNQ (Kv7) potassium channels: physiological regulators and new targets for therapeutic intervention. *Mol. Pharmacol.* 74:1171–1179. https://doi.org/10.1124/mol.108.049825

McCormack, K., L. Lin, L.E. Iverson, M.A. Tanouye, and F.J. Sigworth. 1992. Tandem linkage of Shaker K+ channel subunits does not ensure the stoichiometry of expressed channels. *Biophys. J.* 63:1406–1411. https://doi.org/10.1016/S0006-3495(92)81703-4

Meisel, E., M. Dvir, Y. Haitin, M. Giladi, A. Peretz, and B. Attali. 2012. KCNQ1 channels do not undergo concerted but sequential gating transitions in both the absence and the presence of KCNE1 protein. *J. Biol. Chem.* 287:34212–34224. https://doi.org/10.1074/jbc.M112.364901

Miceli, F., M.V. Soldovieri, M. Martire, and M. Taglialatela. 2008. Molecular pharmacology and therapeutic potential of neuronal Kv7-modulating drugs. *Curr. Opin. Pharmacol.* 8:65–74. https://doi.org/10.1016/j.coph.2007.10.003

Miceli, F., M.R. Cilio, M. Taglialatela, and F. Bezanilla. 2009. Gating currents from neuronal K(V)7.4 channels: general features and correlation with the ionic conductance. *Channels (Austin).* 3:277–283. https://doi.org/10.4161/chan.3.4.9477

Miceli, F., M.V. Soldovieri, F.A. Iannotti, V. Barrese, P. Ambrosino, M. Martire, M.R. Cilio, and M. Taglialatela. 2011. The Voltage-Sensing Domain of K(v)7.2 Channels as a Molecular Target for Epilepsy-Causing Mutations and Anticonvulsants. *Front. Pharmacol.* 2:2. https://doi.org/10.3389/fphar.2011.00002

Miceli, F., M.V. Soldovieri, P. Ambrosino, V. Barrese, M. Migliore, M.R. Cilio, and M. Taglialatela. 2013. Genotype-phenotype correlations in neonatal epilepsies caused by mutations in the voltage sensor of K(v)7.2 potassium channel subunits. *Proc. Natl. Acad. Sci. USA.* 110:4386–4391. https://doi.org/10.1073/pnas.1216867110

Miceli, F., M.V. Soldovieri, P. Ambrosino, L. Manocchio, A. Medoro, I. Mosca, and M. Taglialatela. 2017. Pharmacological targeting of neuronal Kv7.2/3 channels: A focus on chemotypes and receptor sites. *Curr. Med. Chem.* 25:2637–2660. https://doi.org/10.2174/0929867324666171012122852

Osteen, J.D., R. Barro-Soria, S. Robey, K.J. Sampson, R.S. Kass, and H.P. Larsson. 2012. Allosteric gating mechanism underlies the flexible gating of KCNQ1 potassium channels. *Proc. Natl. Acad. Sci. USA.* 109:7103–7108. https://doi.org/10.1073/pnas.1201582109

Padilla, K., A.D. Wickenden, A.C. Gerlach, and K. McCormack. 2009. The KCNQ2/3 selective channel opener ICA-27243 binds to a novel voltage-sensor domain site. *Neurosci. Lett.* 465:138–142. https://doi.org/10.1016/j.neulet.2009.08.071

Peretz, A., L. Pell, Y. Gofman, Y. Haitin, L. Shamgar, E. Patrich, P. Kornilov, O. Gourgy-Hacohen, N. Ben-Tal, and B. Attali. 2010. Targeting the voltage sensor of Kv7.2 voltage-gated K+ channels with a new gating-modifier. *Proc. Natl. Acad. Sci. USA.* 107:15637–15642. https://doi.org/10.1073/pnas.0911294107

Porter, R.J., A. Partiot, R. Sachdeo, V. Nohria, and W.M. Alves. 205 Study Group. 2007. Randomized, multicenter, dose-ranging trial of retigabine for partial-onset seizures. *Neurology.* 68:1197–1204. https://doi.org/10.1212/01.wnl.0000259034.45049.00

Sack, J.T., O. Shamotienko, and J.O. Dolly. 2008. How to validate a heteromeric ion channel drug target: assessing proper expression of concatenated subunits. *J. Gen. Physiol.* 131:415–420. https://doi.org/10.1085/jgp.200709939

Schenzer, A., T. Friedrich, M. Pusch, P. Saftig, T.J. Jentsch, J. Grötzinger, and M. Schwake. 2005. Molecular determinants of KCNQ (Kv7) K+ channel sensitivity to the anticonvulsant retigabine. *J. Neurosci.* 25:5051–5060. https://doi.org/10.1523/JNEUROSCI.0128-05.2005

Shih, T.M., R.D. Smith, L. Toro, and A.L. Goldin. 1998. High-level expression and detection of ion channels in Xenopus oocytes. *Methods Enzymol.* 293:529–556. https://doi.org/10.1016/S0076-6879(98)93032-4

Suh, B.C., and B. Hille. 2007. Regulation of KCNQ channels by manipulation of phosphoinositides. *J. Physiol.* 582:911–916. https://doi.org/10.1113/jphysiol.2007.132647

Suh, B.C., T. Inoue, T. Meyer, and B. Hille. 2006. Rapid chemically induced changes of PtdIns(4,5)P2 gate KCNQ ion channels. *Science.* 314:1454–1457. https://doi.org/10.1126/science.1131163

Sun, J., and R. MacKinnon. 2017. Cryo-EM Structure of a KCNQ1/CaM Complex Reveals Insights into Congenital Long QT Syndrome. *Cell.* 169:1042–1050.e9. https://doi.org/10.1016/j.cell.2017.05.019

Telezhkin, V., D.A. Brown, and A.J. Gibb. 2012. Distinct subunit contributions to the activation of M-type potassium channels by PI(4,5)P2. *J. Gen. Physiol.* 140:41–53. https://doi.org/10.1085/jgp.201210796

Wainger, B.J., E. Kiskinis, C. Mellin, O. Wiskow, S.S. Han, J. Sandoe, N.P. Perez, L.A. Williams, S. Lee, G. Boulting, et al. 2014. Intrinsic membrane hyperexcitability of amyotrophic lateral sclerosis patient-derived motor neurons. *Cell Reports.* 7:1–11. https://doi.org/10.1016/j.celrep.2014.03.019

Wang, A.W., R. Yang, and H.T. Kurata. 2017. Sequence determinants of subtype-specific actions of KCNQ channel openers. *J. Physiol.* 595:663–676. https://doi.org/10.1113/JP272762

Werry, D., J. Eldstrom, Z. Wang, and D. Fedida. 2013. Single-channel basis for the slow activation of the repolarizing cardiac potassium current, I(Ks). *Proc. Natl. Acad. Sci. USA.* 110:E996–E1005. https://doi.org/10.1073/pnas.1214875110

Xiong, Q., H. Sun, and M. Li. 2007. Zinc pyrithione-mediated activation of voltage-gated KCNQ potassium channels rescues epileptogenic mutants. *Nat. Chem. Biol.* 3:287–296. https://doi.org/10.1038/nchembio874

Xiong, Q., Z. Gao, W. Wang, and M. Li. 2008. Activation of Kv7 (KCNQ) voltage-gated potassium channels by synthetic compounds. *Trends Pharmacol. Sci.* 29:99–107. https://doi.org/10.1016/j.tips.2007.11.010

Yau, M.C., R.Y. Kim, C.K. Wang, J. Li, T. Ammar, R.Y. Yang, S.A. Pless, and H.T. Kurata. 2018. One drug-sensitive subunit is sufficient for a near-maximal retigabine effect in KCNQ channels. *J. Gen. Physiol.* https://doi.org/10.1085/jgp.201812013

Yu, H., M. Wu, S.D. Townsend, B. Zou, S. Long, J.S. Daniels, O.B. McManus, M. Li, C.W. Lindsley, and C.R. Hopkins. 2011. Discovery, Synthesis, and Structure Activity Relationship of a Series of N-Aryl-bicyclo[2.2.1] heptane-2-carboxamides: Characterization of ML213 as a Novel KCNQ2 and KCNQ4 Potassium Channel Opener. *ACS Chem. Neurosci.* 2:572–577. https://doi.org/10.1021/cn200065b

Zaydman, M.A., and J. Cui. 2014. PIP2 regulation of KCNQ channels: biophysical and molecular mechanisms for lipid modulation of voltage-dependent gating. *Front. Physiol.* 5:195. https://doi.org/10.3389/fphys.2014.00195

Zaydman, M.A., J.R. Silva, K. Delaloye, Y. Li, H. Liang, H.P. Larsson, J. Shi, and J. Cui. 2013. Kv7.1 ion channels require a lipid to couple voltage sensing to pore opening. *Proc. Natl. Acad. Sci. USA.* 110:13180–13185. https://doi.org/10.1073/pnas.1305167110